BMC Genomics

RESEARCH Open Access

Transcriptomics insights into glutamine on repairing of histamine-induced Yak rumen epithelial cells barrier damage in vitro

Xiaohong Zhang[1†], Rui Hu[1†], Zhisheng Wang[1*], Junmei Wang[1], Ziqi Yue[1], Fali Wu[1], Wenjuan Zhou[1] and Ali Mujtaba Shah[2]

Abstract

Background Glutamine (Gln) plays a pivotal role in maintaining the integrity of the rumen epithelial barrier in mammals. This study aimed to investigate the effects of Gln on histamine-induced barrier damage in yak rumen epithelial cells (YRECs).

Results RT-qPCR analysis revealed a significant decrease in the mRNA expression of tight junction proteins (*ZO-1*, *JAM-A*, *Claudin-1*, and *Claudin-4*) following 24-hour exposure to 20 μM histamine (HIS group) ($P < 0.05$). In the subsequent experiment, YRECs were first treated with 20 μM histamine for 24 h, followed by 8 mM glutamine for 12 h (HG group). Gln treatment reversed the histamine-induced downregulation of both mRNA and protein levels of tight junction proteins and restored the distribution of ZO-1 at the cell membrane. Transcriptome analysis revealed that co-regulated differentially expressed genes were primarily involved in the mitogen-activated protein kinase (MAPK) signaling pathway and apoptosis. These findings were further corroborated by RT-qPCR, Western blot, and flow cytometry analyses. To determine whether glutamine regulates cell barrier function through the p38 MAPK signaling pathway, 20 μM Skatole, a p38 MAPK agonist, was introduced (SK group). The results showed a significant increase in the p-p38/p38 ratio and a marked decrease in the mRNA and protein expression of tight junction proteins in the SK group compared to the HG group ($P < 0.05$).

Conclusions Glutamine mitigates histamine-induced barrier damage in YRECs through the p38 MAPK signaling pathway and apoptosis regulation.

Keywords Histamine, Glutamine, Tight junction, RNA-seq, Yak

†Xiaohong Zhang and Rui Hu contributed equally to this work.

*Correspondence:
Zhisheng Wang
zswangsicau@126.com
[1]Low Carbon Breeding Cattle and Safety Production University Key Laboratory of Sichuan Province, Sichuan Agriculture University, Chengdu 611130, China
[2]Key Laboratory of Animal Genetics, Breeding and Reproduction of Shanxi Province, College of Animal Science and Technology, Northwest A&F University, Yangling 712100, China

Introduction

The unique characteristics of yaks suggest significant potential for the future development of yak-derived milk and meat products. To advance the yak industry, improving growth rates, production performance, and herd size is crucial. The breeding model has shifted toward large-scale, centralized breeding with high-concentrate diets to enhance production performance. However, excessive intake of high concentrate diet often leads to numerous illnesses issues. Subacute rumen acidosis (SARA), a common nutritional disorder characterized by a lowered rumen pH [1], induces microbial death and endotoxin release [2], resulting in increased rumen epithelial permeability and dysfunction [3, 4]. Consequently, harmful substances enter the bloodstream, triggering pathological responses [5]. The rumen epithelium plays a vital role not only in nutrient absorption but also in preventing harmful materials from entering the bloodstream [6, 7]. Therefore, maintaining the integrity of the rumen epithelium is essential for ruminants [8]. Studies have shown that SARA disrupts rumen epithelial barrier function, posing a threat to animal welfare and ultimately decreasing production efficiency [9, 10]. This highlights the need for research into the detrimental effects of SARA and the development of effective prevention strategies.

SARA induces several complex changes in the rumen, including ruminal hyperosmolarity, increased concentrations of short-chain fatty acids, elevated levels of lipopolysaccharides and histamine, and a reduced pH [11–15]. Recent studies have explored the regulation of the rumen at both the tissue and cellular levels, using single-factor or free-combination approaches [16–19]. However, most research on histamine has focused on macro-level effects, which lacks specificity and depth. Furthermore, limited micro-level research has been conducted in this area, underscoring the need for more detailed molecular level investigations.

At the tissue level, existing studies have demonstrated that histamine can disrupt the rumen barrier by altering barrier permeability (e.g., Isc, Gt, FITC apparent permeability coefficient) and the expression of tight junction (TJ) genes and proteins [16, 20]. Steele et al. [5] further confirmed that during SARA, desmoglein gene expression in rumen tissue is significantly downregulated, impairing the structural integrity of the rumen epithelium. At the cellular level, Aschenbach et al. [21] found that histamine inhibits cell differentiation, and it has been suggested that histamine can activate the NF-kB pathway to mediate inflammation [22]. Wang et al. [23] demonstrated that high histamine levels inhibit autophagy in cells. However, the exact effect of histamine on rumen epithelial cell barrier function remains unclear, warranting further exploration at the cellular level.

Glutamine promotes growth, enhances immune function, acts as an antioxidant, and is particularly effective in repairing the gastrointestinal tract [24–26]. Ma et al. [27] showed that glutamine supplementation reduces markers of intestinal permeability and increases rumen height and surface area in stunted yaks, suggesting that dietary glutamine can improve gastrointestinal barrier function. This study aims to investigate the impact of histamine on the rumen epithelial cell barrier and explore the mechanisms through which glutamine mitigates histamine-induced disruption of the rumen epithelial barrier in yaks.

Methods

Cell culture and treatments

YRECs were provided by the rumination research group at the Institute of Animal Nutrition, Sichuan Agricultural University, China, as reported by Wang et al. [28]. The animal study protocol was approved by the Animal Policy and Welfare Committee of the Agricultural Research Organization of Sichuan Province, China, and complied with the guidelines of the Animal Care and Ethical Committee of Sichuan Agricultural University (protocol code SCAUAC2021-36, approved on 29 August 2021). In vitro immortalized YRECs were successfully obtained and identified through Immunofluorescence Identification. The YRECs were cultured in DMEM medium containing 10% fetal bovine serum (Cell-Box, Hong Kong, China) and 1% Pen-Strep Amphotericin B Solution (VivaCell, Shanghai, China).

Cells were incubated under three conditions: without histamine (CON), with 20 μM histamine for 24 h (HIS) based on our preliminary experiments, or with 20 μM histamine for 24 h followed by 8 mM glutamine for 12 h (HG). For pathway validation, cells were treated with 20 μM histamine for 24 h, followed by 8 mM glutamine and 20 μM Skatole for 6 h, then 8 mM glutamine for an additional 6 h (SK). Skatole (MedChemExpress, USA), a p38 MAPK activator, modulates intestinal epithelial cell functions by stimulating aromatic hydrocarbon receptors and p38 [29]. The Skatole concentration used in this study was confirmed to be non-cytotoxic in cell viability assays (Supplement diagram 1), without inducing adverse effects on the cells.

Cell viability test

For cell viability assays, YRECs were seeded in 96-well plates at a density of 1×10^3 cells per well. Five biological replicates were performed for each experimental treatment. Cell viability was assessed using the Cell Counting Kit-8 (CCK-8; Oriscience, China) according to the manufacturer's instructions. Briefly, 100 μL of culture medium was removed, and one-tenth of the volume of CCK-8 reagent was added to the medium. After incubating at

37 °C for 1 h, absorbance was measured at 450 nm using a microplate reader (SpectraMax M2, USA).

Cell proliferation

EDU assays were performed in accordance with the manufacturer's instructions using the EDU Cell Proliferation Assay Kit. Briefly, EDU solution was added to cell culture plates and incubated at 37 °C with 5% CO_2 for 1 h. Following incubation, cells were fixed with 4% paraformaldehyde, permeabilized with 0.2% Triton X-100, and incubated with the click reaction mixture for 1.5 h at room temperature, shielded from light. After counterstaining with DAPI for 10 min, fluorescence images were acquired using a Leica fluorescence microscope (Leica, Wetzlar, Germany). Each treatment group included three biological replicates.

Table 1 Primers used for quantitative real-time PCR (RT-qPCR)

Primers	Primer sequences (5′-3′)[1)]	Product sizes (bp)
ZO-1	F: CCGAATGAAACCGCACACAAACC	107
	R: GTCTCCACGCCACTGTCAAACTC	
Occludin	F: GCCTGTGTTGCCTCCACTCTTG	143
	R: CCATAGCCATAACCGTAGCCATAGC	
JAM-A	F: GTGCCTCCATCCAAGCCTACAATC	134
	R: GGCATCTCTACTCCATCCTTGAACC	
Cluadin-4	F: TCATCGGCAGCAACATCGTCAC	110
	R: CAGCAGCGAGTCGTACACCTTG	
Cluadin-1	F: CCCGTGCCTTGATGGTGATTGG	110
	R: CATCTTCTGTGCCTCGTCGTCTTC	
KITLG	F: CCGTAGCATTGCCAGCATTC	56
	R: AAAGGCCCCAAAAGCAAACC	
FGF7	F: ATGTGAACTGTTCCAGCCCC	192
	R: TTCCAACAGCCACTGTCCTG	
HGF	F: TTTGCCTTCGAGCTATCGGG	225
	R: TGATCCCAGCGCTGACAAAT	
PIK3CA	F: CAATCGGTGACTGTGTGGGA	119
	R: CTGATGGAGTGTGTGGCTGT	
MAPK9	F: GCACCCTGAAGATCCTCGAC	126
	R: TCTCTTTGTAGCCCATGCCC	
BIRC3	F: CCAGCTTGGAAAACAGTGGC	199
	R: GCTTTTGCCAGGTCTGTTGG	
AKT3	F: TGTGGATTTACCTTATCCCCTCA	79
	R: GTTTGGCTTTGGTCGTTCTGT	
KRAS	F: ACATTGGTGAGAGAGATCCGA	70
	R: CACAGCCAGGAGTCTTTTCTTC	
SOS1	F: CAAGTTCACCCTACTCTTGAGTC	172
	R: CATCAGCTATTGCCCACTTATCA	
FOS	F: CGGGTTTCAACGCCGACTA	166
	R: TTGGCACTAGAGACGGACAGA	
XIAP	F: CGAGCTGGGTTTCTTTATACCG	126
	R: GCAATTTGGGGATATTCTCCTGT	
Caspase-1	F: GGATGGGATCTGCGGGACTATG	96
	R: CTGAGGCAATTACGGTTGTTGAATG	
Caspase-9	F: CGAGACCCTGGACAGCATTT	116
	R: AGCCCGGCATCTGTTTGTAA	
BAX	F: TGCTTCAGGGTTTCATCCAGGG	328
	R: GTCCTGATCAACTCGGGCAC	
Bcl2	F: ATGTGTGTGGAGAGCGTCAA	190
	R: GTGCCTTCAGAGACAGCCAG	
GAPDH	F: CGGCACAGTCAAGGCAGAGAAC	116
	R: CCACATACTCAGCACCAGCATCAC	

[1)] F, forward primer; R, reverse primer

Apoptosis detection by flow cytometry

Cells from each treatment group were stained with Annexin-V-FITC and PI using apoptosis kits (DOJINDO, AD10, Japan), adhering to the manufacturer's protocol. Each treatment group consisted of six biological replicates, with the cell concentration in each tube exceeding 1×10^6 cells/ml. Annexin V specifically labels early apoptotic cells by binding to externalized phosphatidylserine on the cell membrane, emitting green fluorescence. PI, which only enters cells with compromised membranes (indicative of late apoptosis or necrosis), emits red fluorescence. In late-stage apoptosis or necrosis, both Annexin V and PI penetrate the cell membrane, resulting in dual red and green fluorescence. After dark incubation for 15 min, cell staining was analyzed using a flow cytometer. Detection was performed with an excitation wavelength of 488 nm and an emission wavelength of 530 nm.

RNA extraction and quantitative real-time PCR (RT-qPCR)

Total RNA from YRECs in each treatment group was isolated using AG RNAex Pro Reagent (AG, China) following the manufacturer's protocol. Reverse transcription was conducted to synthesize cDNA using ExonScript RT SuperMix with dsDNase (EXONGEN, Chengdu, China). Quantitative RT-PCR (RT-qPCR) was carried out using the 2x Universal Blue SYBR Green qPCR Master Mix kit (Servicebio, G3326, China) and analyzed with the QuantStudio™ 5 real-time PCR system (Applied Biosystems, Thermo Fisher Scientific). Primer sequences are provided in Table 1. The PCR cycling conditions included an initial 30-second denaturation at 95 °C, followed by 40 cycles of 15-second denaturation at 95 °C, 10-second annealing at 60 °C, and 30-second extension at 72 °C. Each treatment group included six biological replicates. Relative mRNA expression levels were quantified using the $2^{-\Delta\Delta CT}$ method and normalized to the geometric mean of GAPDH.

Western blot analysis

YREC protein lysates from each treatment group were harvested using the ExKine™ Pro Total Protein Extraction Kit for Animal Cultured Cells and Tissues (Abbkine), and protein concentration was quantified using the BCA assay kit (Abbkine). Equal amounts of protein lysates were separated by 7.5% SDS-PAGE (Epizyme, Shanghai, China). Each treatment group consisted of three

biological replicates, with each well representing one replicate. After electrophoresis, gels were excised based on the protein size indicated by the Marker (LABLEAD, P10310, China) before proceeding to the transfer step. Proteins were transferred onto PVDF membranes (Bio-RAD, USA). Blocking was performed with protein-free rapid blocking buffer (Servicebio, G2052, China) for 10 min, followed by overnight incubation at 4 °C with primary antibodies: anti-ZO-1 (1:2000, Proteintech, USA), anti-JAM-A (1:1000, ABclonal, USA), anti-Claudin-1 (1:1000, Proteintech, USA), anti-Claudin-4 (1:1000, Proteintech, USA), anti-Occludin (1:1000, ABclonal, USA), anti-GAPDH (1:1000, ABclonal, USA), anti-p38 (1:1000, ABclonal, USA), anti-p-p38 (1:1000, ABclonal, USA), anti-ERK (1:1000, ABclonal, USA), anti-p-ERK (1:1000, ABclonal, USA), anti-JNK (1:1000, ABclonal, USA), and anti-p-JNK (1:2000, ABclonal, USA). GAPDH served as the internal control for total protein. Following this, secondary antibody incubation was performed for 1.5 h. Protein bands were visualized using an e-Blot Touch Imager (e-Blot, USA) with the Oriscience Supersensitive ECL Kit (Oriscience, China). As the gels were cropped prior to the transfer step, full-length blot images are not available.

Immunofluorescence detection of ZO-1

Cells from each group were washed three times with PBS for 5 min per wash. They were then fixed with 75% ethanol for 20 min and permeabilized with 0.2% Triton X-100 for 20 min. After blocking with goat serum for 1 h, cells were incubated with primary antibody (ZO-1, 1:150) overnight at 4 °C. Following secondary antibody incubation for 2 h, DAPI was added dropwise and incubated for 5 min in the dark. The PBS was removed, and an anti-fluorescence quencher was added. Each treatment group comprised five biological replicates. Fluorescence microscopy was used for imaging, and ImageJ was employed for analysis.

RNA-Seq assay and data analysis

Each experimental group included four independent biological replicates. Library construction was performed using the Illumina HiSeq 2500 platform from Genedenovo Biotechnology Co., followed by sequencing. HISAT2 was employed to align the reads to the TAIR 10 genome [30]. Differentially expressed genes (DEGs) were identified using DESeq2, with a threshold of an absolute fold change > 2 and a *P*-value < 0.05 [31]. Enriched metabolic pathways were determined through Gene Ontology (GO) and Kyoto Encyclopedia of Genes and Genomes (KEGG) database annotations. Subsequently, DEGs were selected for protein-protein interaction (PPI) network analysis *via* the STRING database (v11.0), and Cytoscape 3.9.1 software was used to visualize and analyze the intricate gene networks.

Statistical analysis

Statistical analyses were conducted using SPSS version 27.0. Data from yak rumen epithelial cells across different groups were analyzed using Student's t-test and one-way ANOVA, with results expressed as means ± standard deviation (SD). Statistical significance was defined at a *P*-value < 0.05.

Results

Histamine effects on the tight junction of YRECs and Glutamine effects on YRECs viability and proliferation

To assess whether histamine regulates tight junctional mRNA expression, RT-qPCR was performed to measure the levels of TJ proteins. Figure 1A shows a significant reduction in the mRNA levels of TJ proteins (*Claudin-1*, *Claudin-4*, *ZO-1*, and *JAM-A*) in YRECs treated with 20 μM histamine compared to the control group ($P < 0.05$). To determine the optimal concentration of glutamine for YRECs, it was added to the culture medium, and the cells were cultured for 12 h. The 12-hour treatment duration was based on the experimental design outlined by Li et al. [32]. CCK-8 assay results revealed an initial increase in cell viability, followed by a decrease. The highest cell viability was observed at a glutamine concentration of 8 mM (Fig. 1B). Figure 1C illustrates that HIS significantly reduced YREC proliferation compared to the control ($P < 0.05$), while the glutamine repair group (HG) significantly enhanced proliferation relative to the HIS group ($P < 0.05$), suggesting a potential reparative effect of glutamine. Therefore, 8 mM glutamine treatment for 12 h was selected as the optimal condition for repairing cell barrier damage in subsequent experiments.

The expression levels of mRNA and protein of the tight junction proteins in different groups

Figure 2 shows an increase in the mRNA levels of TJ proteins (*Claudin-1*, *Claudin-4*, *ZO-1*, and *JAM-A*) in 20 μM histamine-treated YRECs compared to the control group, while *Occludin* mRNA levels remained unchanged. In the HG group, the mRNA levels of *Claudin-1*, *Claudin-4*, *ZO-1*, *JAM-A*, and *Occludin* were significantly higher than in the HIS group, with some markers also showing significantly higher expression compared to the control group. The protein expression levels of Claudin-1, Claudin-4, ZO-1, and JAM-A aligned with the mRNA expression patterns, while Occludin protein expression did not exhibit significant differences across treatment groups.

Expression and distribution of ZO-1 in different groups

Immunofluorescence analysis revealed that histamine treatment reduced ZO-1 protein abundance and

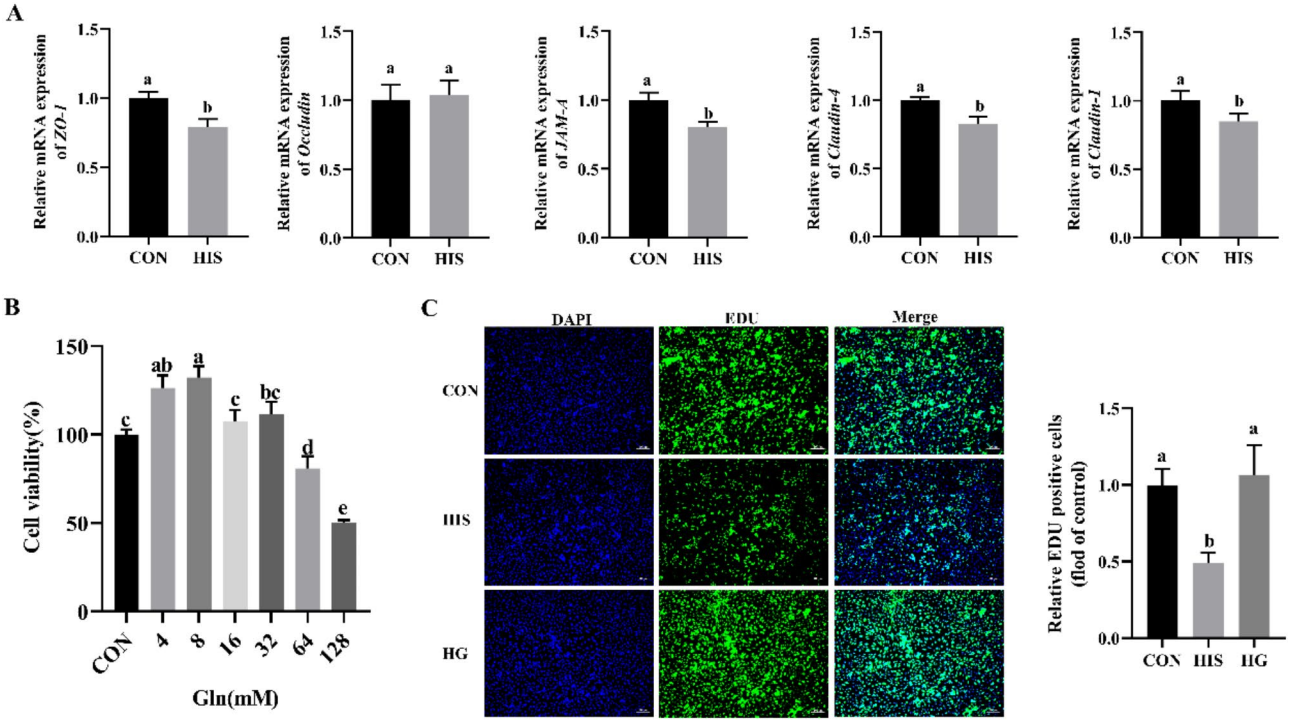

Fig. 1 Effect of histamine on the tight junction of yak rumen epithelial cells (YRECs) and the toxic effect of glutamine on YRECs in vitro. A, YRECs were treated either with 20 μM or without histamine (CON) for 24 h. The mRNA levels of the ZO-1, Occludin, JAM-A, Claudin-4, and Claudin-1 genes in the histamine-treated YRECs were measured by RT-qPCR. B, Cell viability of YRECs after glutamine treatment (4, 8, 16, 32, 64, 128 mM) for 12 h. C, Cell Proliferation of YRECs in different treatment groups. Each treatment group's data were normalized using data from the control group. Different letters indicate significant differences ($P < 0.05$). An independent-sample t-test was used to calculate group-to-group comparisons

disrupted its cellular localization, leading to decreased distribution at the cell membrane and perimembrane regions. In contrast, glutamine treatment restored ZO-1 expression, enhancing its membrane distribution and mitigating histamine-induced cell damage (Fig. 3).

RNA sequencing data

Samples were collected after YRECs were cultured with 20 μM histamine for 24 h followed by 8 mM glutamine treatment for 12 h (HG), or with 20 μM histamine alone for 24 h (HIS), as well as the control group (CON) for RNA sequencing. RNA sequencing data were analyzed to evaluate gene expression levels. The statistical results of gene expression in the different sample groups are presented in the violin plot (Fig. 4A). Principal component analysis (PCA) demonstrated clear clustering of the three sample groups, with relative dispersion shown in Fig. 4B. Correlation analysis indicated that the correlation between samples was approximately 0.9, confirming the reliability of the sample selection (Fig. 4C). The uniformity within each group was satisfactory, meeting the required standards for subsequent experiments. The volcano plot displayed the DEGs, revealing a total of 1861 DEGs in the HIS versus CON comparison, with 249 upregulated and 1612 downregulated genes. In the HG versus HIS comparison, 6351 DEGs were identified, with 3649 upregulated and 2702 downregulated (Fig. 4D, E). A Venn diagram analysis identified 1444 DEGs common to both comparisons, which may play a critical role in the histamine-induced barrier damage in YRECs that is repaired by glutamine treatment (Fig. 4F).

Functional analysis of DEGs

The functional role of the DEGs was further investigated through functional enrichment analysis. Gene Ontology (GO) enrichment analysis revealed that 56 GO terms were significantly enriched ($P < 0.05$). These terms were categorized into three groups: molecular functions (13 GO terms), cellular components (17 GO terms), and biological processes (26 GO terms). The co-regulated DEGs were predominantly enriched in biological processes such as cellular processes, single-organism processes, and metabolic processes. In terms of molecular functions, the DEGs were mainly enriched in binding, catalytic activity, and nucleic acid binding transcription factor activity. For cellular components, DEGs were primarily associated with cells, cell parts, organelles, and other cellular structures (Fig. 4G).

Additionally, KEGG pathway enrichment analysis identified 312 significantly enriched pathways, with the top 20 pathways shown in Fig. 4H. The DEGs were most significantly enriched in pathways such as the MAPK

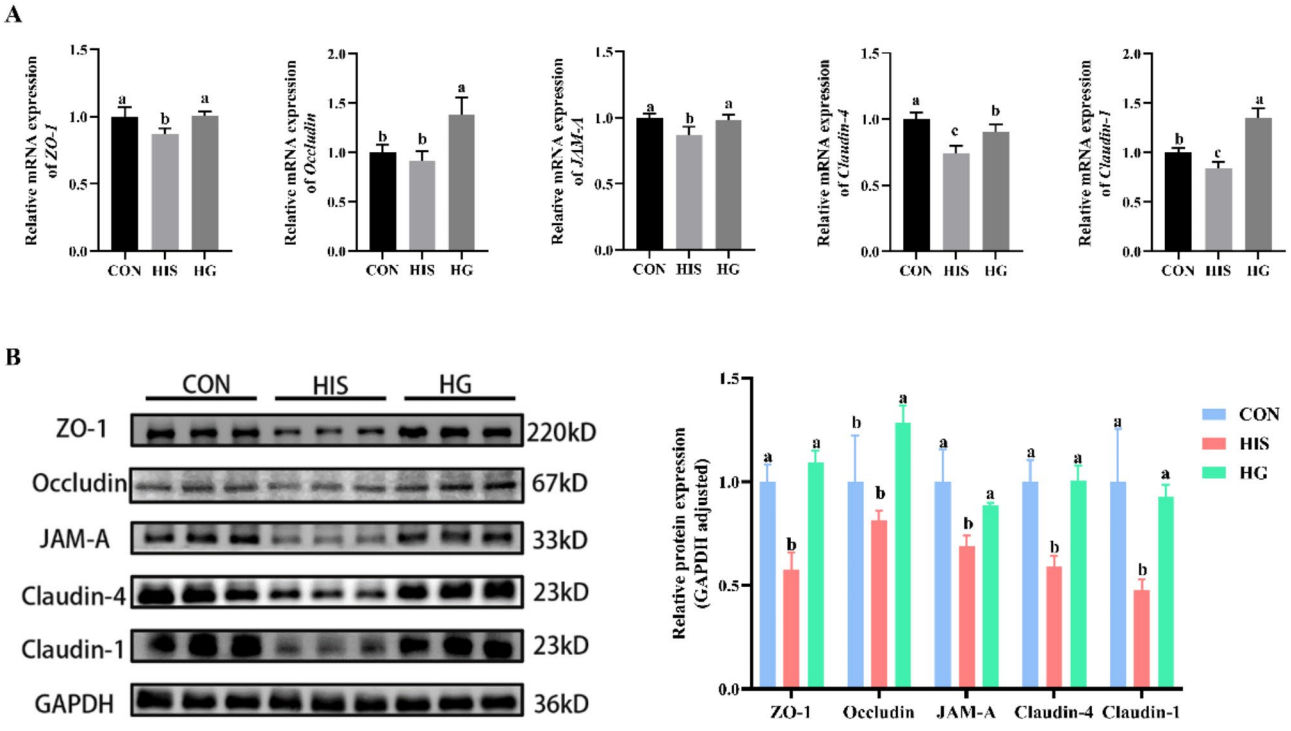

Fig. 2 The expression levels of mRNA and protein of the tight junction proteins in different groups. **A**, the relation mRNA expression levels of the *Claudin-1*, *Claudin-4*, *ZO-1*, *JAM-A*, *Occludin* genes in different treatment groups. **B**, the relation protein levels of the Claudin-1, Claudin-4, ZO-1, JAM-A, Occludin genes in different treatment groups. Band intensities were quantified by Image J and normalized to GAPDH. All results are shown as mean ± SD. Different letters indicate significant differences ($P < 0.05$)

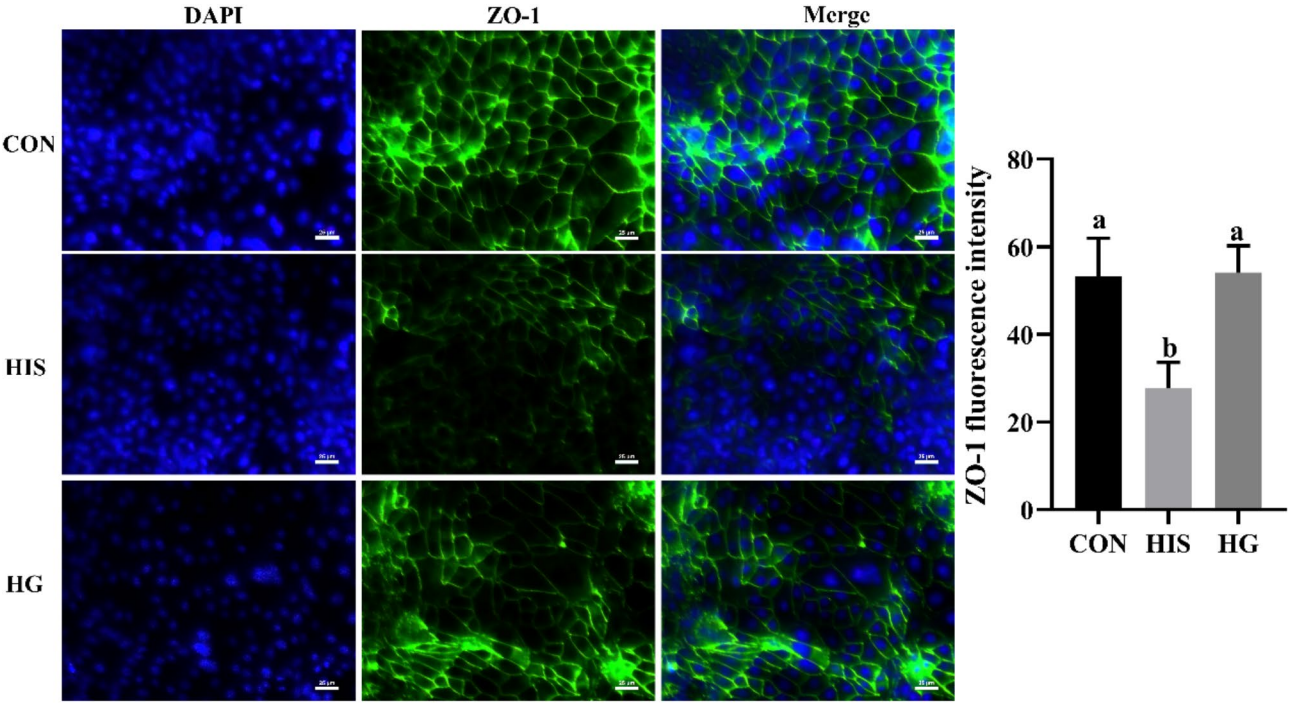

Fig. 3 Effect of Gln on the expression and distribution of ZO-1 in histamine-damaged YRECs. DAPI labeled nucleus as blue, ZO-1 stained as green. Scale bars represent 25 μm. Mean ± SD data are presented. Different letters indicate significant differences ($P < 0.05$). Each treatment group's data were normalized using data from the control group

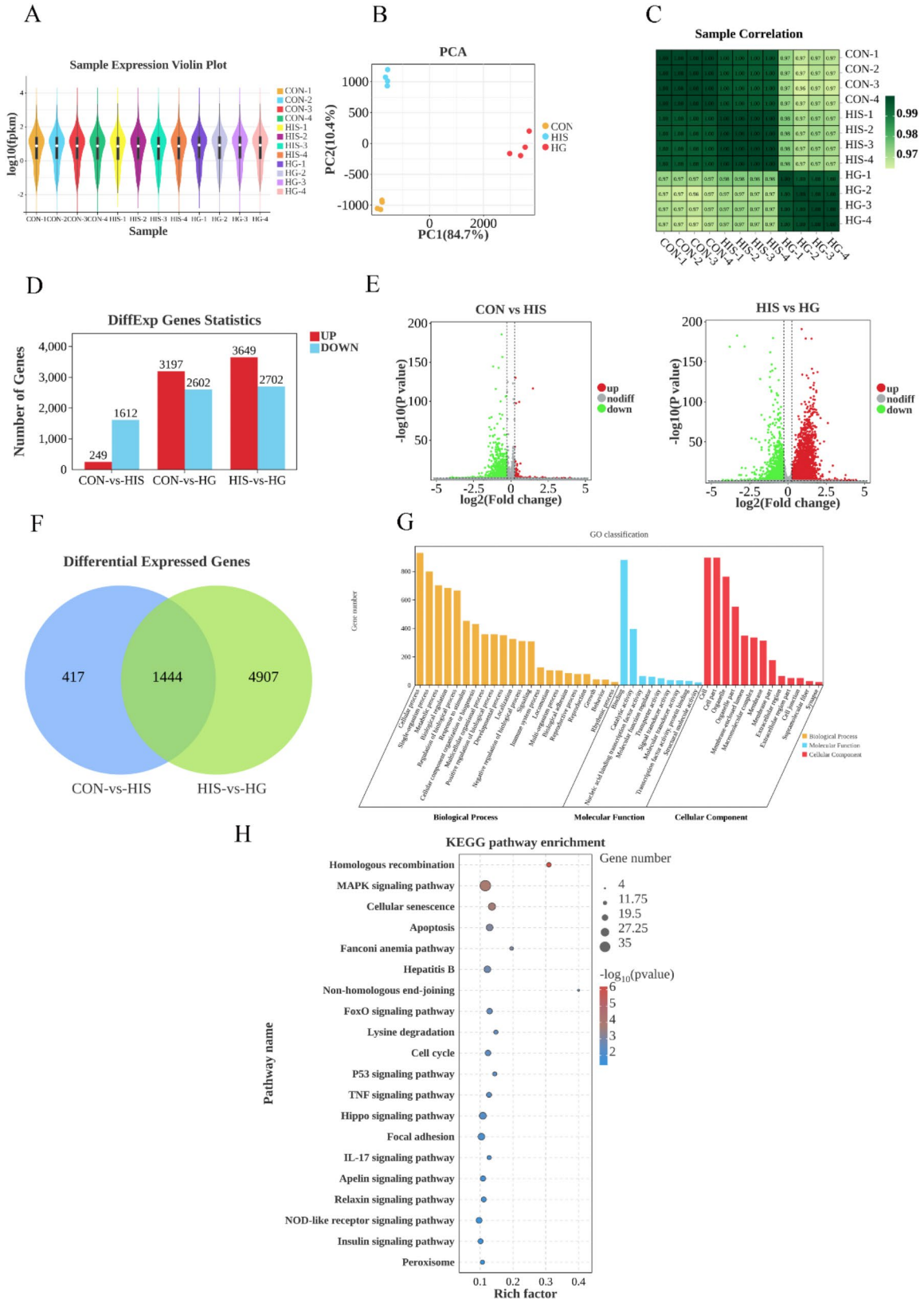

Fig. 4 The RNA-sequencing analysis of different treatment groups. **A**, sample expression violin plot. **B**, principal component analysis of a sample. **C**, sample correlation heatmap. **D**, statistical chart of differentially expressed genes (DEGs). **E**, volcano map of differentially expressed genes (DEGs). **F**, venn diagram of differentially expressed genes (DEGs). **G**, GO enrichment classification histogram. **H**, KEGG enrichment bubble plot. The data presented are from four independent experiments ($n = 4$)

signaling pathway, cellular senescence, apoptosis, FoxO signaling pathway, lysine degradation, cell cycle, p53 signaling pathway, TNF signaling pathway, and IL-17 signaling pathway. The two most significant pathways associated with glutamine repair of histamine-induced barrier damage in YRECs were the MAPK signaling pathway ($P = 0.000136$) and apoptosis ($P = 0.000758$).

Identification of DEGs

To further investigate the roles of DEGs in the MAPK and apoptosis signaling pathways, PPI networks were generated using the STRING database and visualized in Cytoscape (Fig. 5A). Eleven core genes (*FGF7*, *KITLG*, *KRAS*, *PIK3CA*, *MAPK9*, *BIRC3*, *AKT3*, *HGF*, *XIAP*, *FOS*, *SOS1*) were selected for RT-qPCR validation. The results from RT-qPCR showed consistent trends with the transcriptome sequencing data, further confirming the reliability of the RNA-seq results (Fig. 5B).

Further analysis of the apoptosis-related genes, based on RNA-seq and existing literature, revealed that the HIS group exhibited a significant increase in the mRNA expression of pro-apoptotic genes and a decrease in the expression of anti-apoptotic genes compared to the CON group. In contrast, the HG group showed a significant reduction in pro-apoptotic gene expression and an increase in anti-apoptotic gene expression compared to the HIS group (Fig. 5C). Flow cytometry results supported these observations, with a marked increase in the percentage of apoptotic cells in the HIS group compared to the CON group, and a significant reduction in apoptosis in the HG group compared to the HIS group (Fig. 5D).

Western blot analysis of three key downstream signaling molecules—p38, extracellular signal-regulated kinase (ERK), and c-Jun N-terminal kinase (JNK)—showed no significant changes in the ratios of p-ERK/ERK and p-JNK/JNK. However, the ratio of p-p38/p38 was significantly elevated in the HIS group compared to the CON group. In contrast, the p-p38/p38 ratio was significantly reduced in the HG group compared to the HIS group (Fig. 5E).

Glutamine inhibits the p38 MAPK pathway to effect tight junction protein in YRECs

Compared to the HG group, the SK group showed a significant upregulation of the p-p38/p38 ratio and a marked reduction in the mRNA and protein expression levels of TJ proteins (JAM-A, ZO-1, Claudin-1, and Claudin-4), with no significant change in Occludin expression (Fig. 6).

Discussion

SARA leads to elevated levels of rumen histamine, which impairs the ruminal epithelium barrier function in ruminants. This disruption compromises animal health and reduces production performance [33]. Recent studies have demonstrated the beneficial effects of glutamine as a dietary supplement for yaks, particularly in improving gastrointestinal function [27, 34]. As the most abundant free amino acid, glutamine plays a pivotal role in strengthening the intestinal barrier and serves as the principal energy source for rapidly proliferating cells [35]. It is a non-essential amino acid with distinct pharmacological properties and lacks toxic side effects. Glutamine acts as a critical nitrogen donor for cellular metabolism, supporting the function of intestinal, immune, and muscle cells [36]. Furthermore, glutamine and its dipeptides are essential nitrogen sources for gastrointestinal epithelial cells, crucial for maintaining mucosal integrity and stability [37]. Previous studies have demonstrated that glutamine supplementation enhances intestinal barrier integrity by promoting the proliferation of intestinal epithelial cells and stabilizing TJs [38]. In a prior study, glutamine supplementation reduced indicators of intestinal permeability and increased rumen height and surface area in stunted yaks, suggesting that glutamine supplementation can enhance gastrointestinal barrier function [27]. This experiment was designed to explore the potential of glutamine in repairing histamine-induced barrier damage in YRECs.

The ruminal epithelium consists of several layers: the basal layer, spinous layer, granular layer, and stratum corneum. These layers are interconnected by TJs, adhesion junctions, gap junctions, and desmosomes [39]. TJs, located at the apex of cell-cell contacts, play a critical role in establishing and maintaining epithelial barrier function and polarity. TJs are membrane protein complexes that bind adjacent plasma membranes tightly together, creating a selectively permeable barrier to restrict the free diffusion of molecules between cells [40–42]. The TJ complex includes structural proteins like Occludin, Claudin-1, and Claudin-4, functional proteins like ZO-1, and adhesion molecules such as JAM-A [43]. These junctions are essential for maintaining the integrity of the gastrointestinal epithelial barrier [44]. Our experimental results show that histamine treatment led to a marked reduction in the mRNA expression of TJ proteins (*Claudin-1*, *Claudin-4*, *ZO-1*, *JAM-A*), which is consistent with the findings of Gao et al. [16]. When glutamine (Gln) was added to the culture medium as a reparative treatment, the HG group showed a significant increase in the mRNA and protein expression levels of TJ proteins (Claudin-1, Claudin-4, ZO-1, JAM-A, and Occludin) compared to the HIS group. These results are consistent with earlier studies by Li et al. [45] and Shaghaghi et al. [46]. The increase in TJ protein expression suggests that glutamine plays a role in restoring cell barrier function.

Transcriptome analysis was conducted to elucidate the molecular mechanisms underlying the restoration

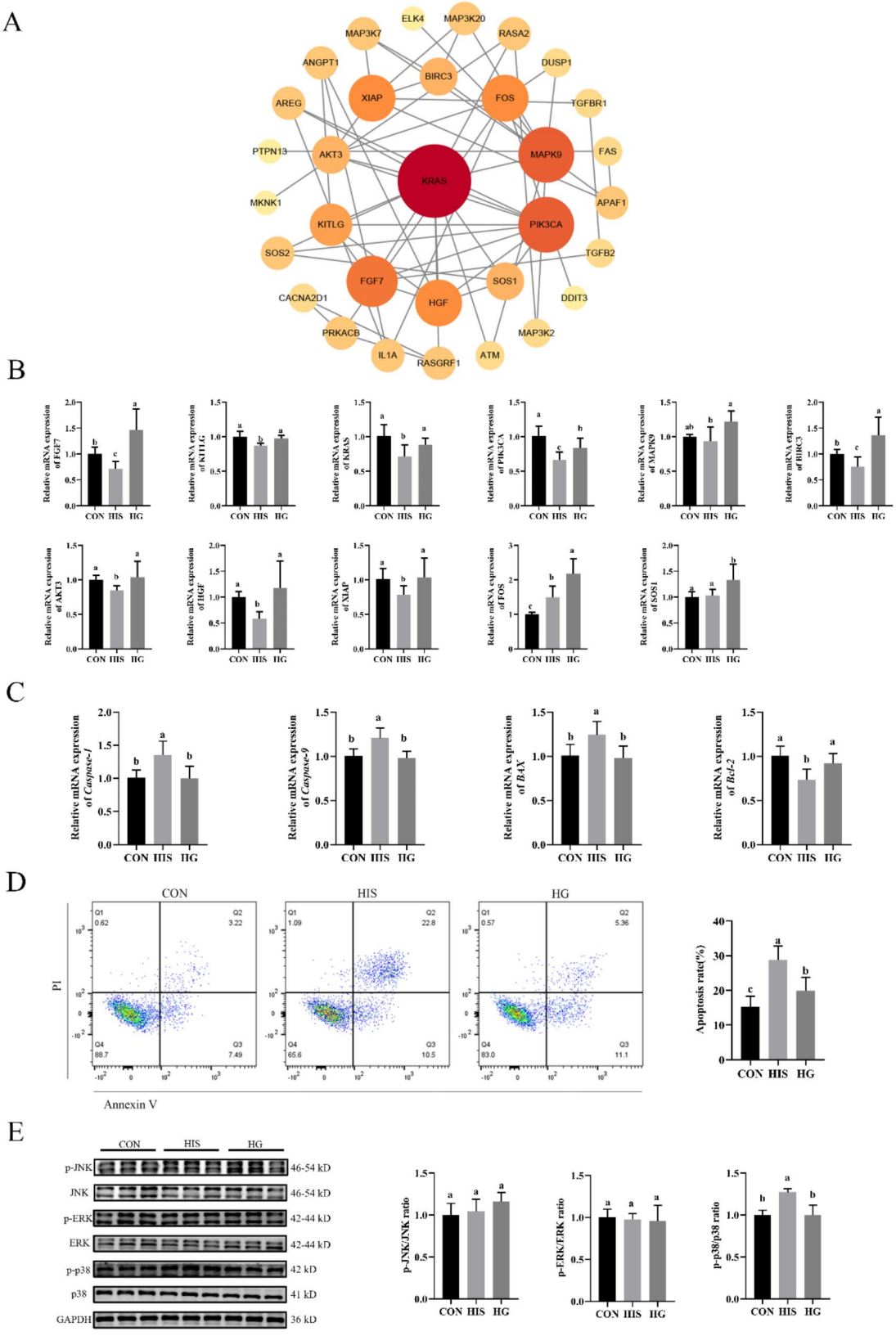

Fig. 5 Validation of the accuracy of RNA sequencing (RNA-Seq). **A**, protein–protein interaction (PPI) networks of the selected differentially expressed genes (DEGs). **B**, the mRNA expression levels of eleven core genes of DEGs. **C**, the mRNA expression levels of genes associated with apoptosis. **D**, cells were exposed to different treatments and were then stained and analyzed by flow cytometry. **E**, the protein expression levels of the MAPK signaling pathway. Different letters indicate significant differences ($P < 0.05$)

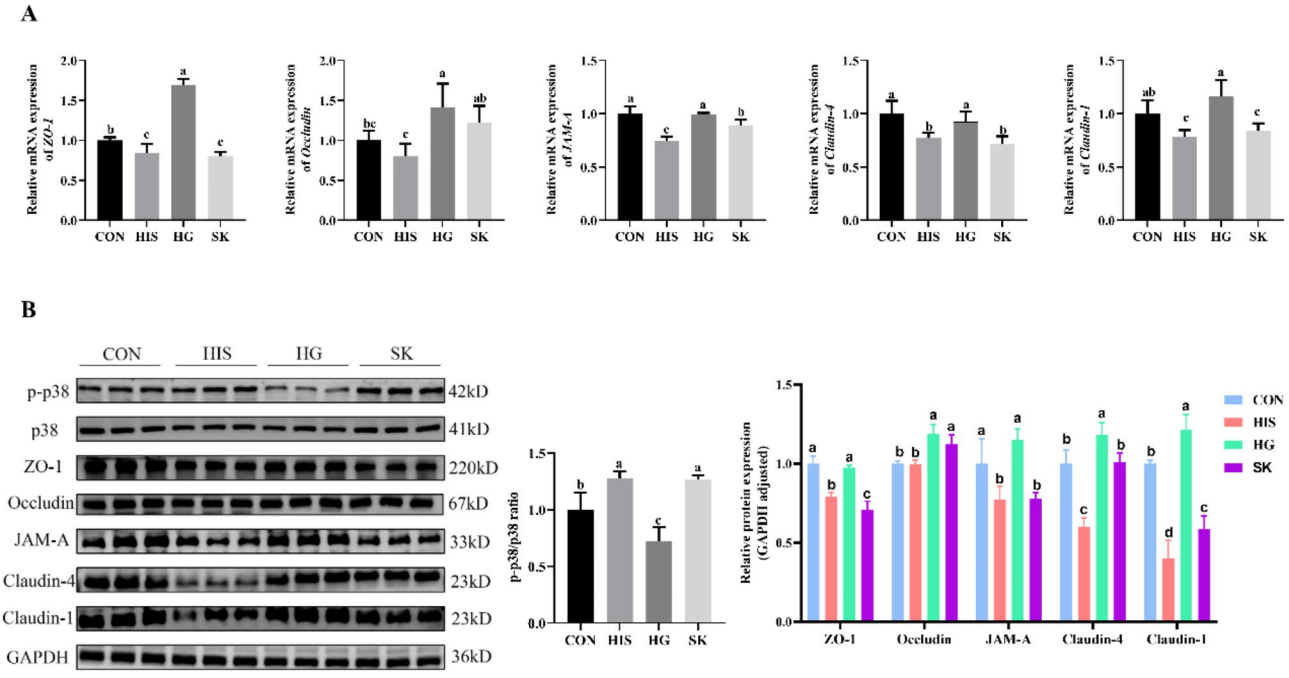

Fig. 6 The expression levels of mRNA and protein of the tight junction and p38 MAPK proteins in different groups. **A**, the mRNA expression levels of the *ZO-1*, *Occludin*, *JAM-A*, *Claudin-4*, *Claudin-1* genes in different treatment groups. **B**, the protein expression levels of the Claudin-1, Claudin-4, ZO-1, JAM-A, Occludin, p38, and p-p38 proteins in different treatment groups. Different letters indicate significant differences ($P < 0.05$)

of YREC barrier function by glutamine. The analysis revealed distinct gene expression profiles among the CON, HIS, and HG groups. KEGG pathway enrichment identified that DEGs were predominantly associated with the MAPK and apoptosis signaling pathways. Transcriptomic data indicated that histamine treatment upregulated DEGs within both the MAPK and apoptosis pathways, while glutamine supplementation led to downregulation of these pathways in the HG group compared to the HIS group. These observations suggest that glutamine may modulate the ruminal epithelial barrier function primarily via the MAPK signaling pathway and apoptosis regulation.

Apoptosis occurs through both extrinsic and intrinsic pathways, with the intrinsic pathway being regulated by the Bcl-2 family, particularly through the interactions between Bcl-2 and Bax. These proteins modulate mitochondrial membrane potential and permeability, facilitating the release of pro-apoptotic factors, which activate initiator caspases, culminating in the activation of executioner caspase-3 [47]. Previous studies have demonstrated that reactive oxygen species (ROS)-mediated epithelial cell apoptosis contributes to intestinal barrier dysfunction in mice [48]. Glutamine supplementation reversed heat stress-induced upregulation of HSP70 expression, apoptosis, and cytosolic cytochrome c levels, while enhancing mitochondrial membrane potential. These observations indicate that glutamine mitigates heat stress-induced TJ damage in porcine intestinal epithelium by inhibiting the HSP70-mediated mitochondrial apoptotic pathway [49]. In this study, RT-qPCR was performed to quantify the mRNA expression levels of apoptosis-related genes (Caspase 1, Caspase 9, Bax, and Bcl-2), while flow cytometry was employed to assess apoptosis rates. Compared to the control group, the histamine-damage group exhibited a reduced mRNA expression of the anti-apoptotic gene *Bcl-2*, alongside an upregulation of pro-apoptotic genes (*Caspase 1*, *Caspase 9*, and *Bax*) and an elevated apoptosis rate. Conversely, the glutamine-repair group demonstrated a decrease in the mRNA levels of pro-apoptotic genes, an increase in the expression of the anti-apoptotic gene Bcl-2, and a lower apoptosis rate. The results of RT-qPCR and flow cytometry were consistent with the findings from transcriptome sequencing. These results suggest that glutamine preserves the integrity of the tight junctions in YRECs via alleviating histamine-induced apoptosis.

The MAPK (Mitogen-Activated Protein Kinase) family consists of at least four subfamilies: Extracellular Signal-Regulated Kinases (ERK1/2), ERK5, c-Jun N-terminal Kinases (JNK1-3), and p38 kinases (p38α, β, γ, and δ). All MAPK signaling pathways are structured around a central three-tier kinase module [50, 51]. The MAPK signaling pathway is typically in a state of dynamic equilibrium under normal, unstimulated conditions. Upon stimulation by various external signals, the MAPK signaling pathway is activated through the phosphorylation of upstream kinases, which subsequently trigger the

activation of MAPKs. This activation leads to the phosphorylation of downstream transcription factors, thereby modulating their biological activity and affecting cellular processes. The activation of this signaling cascade regulates a variety of physiological and pathological processes, including angiogenesis, cell proliferation, differentiation, apoptosis, and tumor metastasis [52]. This study results showed that, compared to the control group, there were no significant changes in p-ERK/ERK and p-JNK/JNK. However, the p-p38/p38 ratio significantly increased after histamine treatment, which is consistent with the findings of Adderley et al. [53]. This suggests that histamine may damage the tight junctions of yak rumen epithelial cells via the p38 MAPK signaling pathway. Moreover, the p-p38/p38 ratio in the HG group significantly decreased compared to the HIS group. Therefore, we hypothesize that glutamine primarily regulates tight junctions in cells through the p38 MAPK signaling pathway. To further validate whether glutamine mediates the regulation of cell barrier function through the p38 MAPK signaling pathway, a p38 agonist was introduced in conjunction with glutamine treatment for 6 h, forming the SK group. The results revealed a significant elevation in the p-p38/p38 ratio in the SK group compared to the HG group, confirming the effective activation of the p38 pathway by the agonist. Additionally, the mRNA and protein levels of TJ proteins (Claudin-1, Claudin-4, ZO-1, JAM-A) were significantly upregulated in the SK group, while Occludin expression remained unchanged. Some TJ proteins in the SK group exhibited notably lower gene and protein expression levels compared to the CON group, suggesting that glutamine regulates the p38 MAPK pathway to mediate cell barrier function.

A limitation of this study is the absence of a glutamine-only treatment group and a p38 MAPK inhibitor group, which could have provided further insights into the individual effects of glutamine and p38 inhibition. Nevertheless, this omission does not undermine the central findings and conclusions of the study, which are supported by consistent trends and robust statistical analyses. While the cell model used in this study offers valuable insights, it may not fully replicate the in vivo conditions. Future investigations for our research group should aim to validate these findings in animal models, considering factors such as immune responses and microbiota interactions. Moreover, transcriptomic data suggest other potential pathways, including FoxO, p53, TNF, and IL-17, which may also contribute to glutamine-mediated repair. Exploring these pathways, along with further validation of DEGs, will provide a more comprehensive understanding of the underlying mechanisms. Additionally, the impact of varying glutamine concentrations on histamine-induced damage was not explored in this study. Proposed future research in our laboratory should investigate the effects of different glutamine concentrations at various time points to further elucidate its repair mechanisms. Despite these limitations, the findings of this study offer valuable insights into glutamine-mediated repair. The proposed future directions will enhance the depth and clinical relevance of this work.

Conclusion

In summary, the study demonstrates that histamine reduces the mRNA and protein levels of TJ proteins in YRECs, impairing barrier integrity. Glutamine treatment effectively repairs histamine-induced barrier damage by reducing apoptosis and modulating the p38 MAPK pathway. These findings provide a theoretical basis for the use of glutamine as a nutritional intervention to alleviate subacute ruminal acidosis caused by intensive feeding practices in yaks raised in high-altitude regions.

Supplementary Information

The online version contains supplementary material available at https://doi.org/10.1186/s12864-025-11383-6.

Supplementary Material 1

Supplementary Material 1

Acknowledgements

We are grateful for the help and support from the bovine low-carbon breeding innovation team of the Animal Nutrition Institute of Sichuan Agricultural University. We are thankful to Guangzhou Genedenovo Biotechnology Co., Ltd. for assisting in sequencing and bioinformatics analysis and sharing their expertise during this research.

Author contributions

ZSW initiated and supervised the project. XHZ and RH performed all libratory experiments and analyzed the data. They also wrote and revised the manuscript. JMW and ZQY collected the cell samples and assisted to perform experiments associated with transcriptomics and immunofluorescence imaging. FLW, WJZ and AMS contributed the idea of manuscript initiation and revised the manuscript. All authors read and approved the final manuscript.

Funding

The authors gratefully acknowledge the National Natural Science Foundation of China (NSFC), Grant/Award Number: 32272909 and the China Agriculture (Beef Cattle/Yak) Research System of MOF and MARA (CARS-37).

Data availability

The datasets generated and analysed during the current study are available in the Genome Sequence Archive repository (GSA: CRA017166), that are publicly accessible at https://ngdc.cncb.ac.cn/gsa.

Declarations

Ethics approval and consent to participate

The use of animals to isolate and develop the cell line was used in the present study was approved by the ethics committee/IRB of Animal Policy and Welfare Committee of the Agricultural Research Organization of Sichuan Province, China. The study is reported in accordance with ARRIVE guidelines (https://arriveguidelines.org).

Consent for publication

Not applicable.

Competing interests
The authors declare no competing interests.

Received: 21 May 2024 / Accepted: 19 February 2025
Published online: 25 February 2025

References

1. Oba M, Allen MS. Effects of brown midrib 3 mutation in corn silage on productivity of dairy cows fed two concentrations of dietary neutral detergent fiber: 3. Digestibility and microbial efficiency. J Dairy Sci. 2000;83(6):1350–8.
2. Chang G, Zhuang S, Seyfert H-M, Zhang K, Xu T, Jin D, Guo J, Shen X. Hepatic TLR4 signaling is activated by LPS from digestive tract during SARA, and epigenetic mechanisms contribute to enforced TLR4 expression. Oncotarget. 2015;6(36):38578–90.
3. Chen M, Xie W, Zhou S, Ma N, Wang Y, Huang J, Shen X, Chang G. A high-concentrate diet induces colonic inflammation and barrier damage in Hu sheep. J Dairy Sci. 2023;106(12):9644–62.
4. Hu H-l, Yang S-q, Cheng M, Song L-w, Xu M, Gao M, Yu Z-t. Long-term effect of subacute ruminal acidosis on the morphology and function of rumen epithelial barrier in lactating goats. J Integr Agric. 2022;21(11):3302–13.
5. Steele MA, Croom J, Kahler M, AlZahal O, Hook SE, Plaizier K, McBride BW. Bovine rumen epithelium undergoes rapid structural adaptations during grain-induced subacute ruminal acidosis. Am J Physiology-Regulatory Integr Comp Physiol. 2011;300(6):R1515–23.
6. Baldwin RL, Connor EE. Rumen function and development. Veterinary Clinics: Food Anim Pract. 2017;33(3):427–39.
7. Baaske L, Gäbel G, Dengler F. Ruminal epithelium: A checkpoint for cattle health. J Dairy Res. 2020;87(3):322–9.
8. Ma J, Shah AM, Wang Z, Fan X. Potential protective effects of thiamine supplementation on the ruminal epithelium damage during subacute ruminal acidosis. Anim Sci J. 2021;92(1):e13579.
9. Grummer RR. Impact of changes in organic nutrient metabolism on feeding the transition dairy cow. J Anim Sci. 1995;73(9):2820–33.
10. Schmitz-Esser S. The rumen epithelial microbiota: possible gatekeepers of the rumen epithelium and its potential contributions to epithelial barrier function and animal health and performance. Meat Muscle Biology. 2021;4(2):1–11.
11. Ametaj BN, Zebeli Q, Saleem F, Psychogios N, Lewis MJ, Dunn SM, Xia J, Wishart DS. Metabolomics reveals unhealthy alterations in rumen metabolism with increased proportion of cereal grain in the diet of dairy cows. Metabolomics. 2010;6(4):583–94.
12. Hernandez J, Benedito JL, Abuelo A, Castillo C. Ruminal acidosis in feedlot: from aetiology to prevention. TheScientificWorldJournal. 2014;2014:702572–702572.
13. Humer E, Aschenbach JR, Neubauer V, Kroeger I, Khiaosa-ard R, Baumgartner W, Zebeli Q. Signals for identifying cows at risk of subacute ruminal acidosis in dairy veterinary practice. J Anim Physiol Anim Nutr. 2018;102(2):380–92.
14. Owens FN, Secrist DS, Hill WJ, Gill DR. Acidosis in cattle: a review. J Anim Sci. 1998;76(1):275–86.
15. Pilachai R, Schonewille JT, Thamrongyoswittayakul C, Aiumlamai S, Wachirapakorn C, Everts H, Hendriks WJLS. Starch source in high concentrate rations does not affect rumen pH, Histamine and lipopolysaccharide concentrations in dairy cows. Livest Sci. 2012;150(1–3):135–42.
16. Gao S, Zhula A, Liu W, Lu Z, Shen Z, Penner GB, Ma L, Bu D. Direct effect of lipopolysaccharide and Histamine on permeability of the rumen epithelium of steers ex vivo. J Anim Sci. 2022;100(2):skac005.
17. He B, Fan Y, Zhao X, Wang H. Lactate transport and metabolism in rumen epithelial cells in SARA condition. Italian J Anim Sci. 2023;22(1):239–49.
18. Lian H, Zhang C, Liu Y, Li W, Fu T, Gao T, Zhang L. In vitro gene expression responses of bovine rumen epithelial cells to different pH stresses. Animals. 2022;12(19):2621.
19. Penner GB, Steele MA, Aschenbach JR, McBride BW. RUMINANT NUTRITION SYMPOSIUM: molecular adaptation of ruminal epithelia to highly fermentable diets. J Anim Sci. 2011;89(4):1108–19.
20. Aschenbach J, Gäbel G. Effect and absorption of Histamine in sheep Rumen: significance of acidotic epithelial damage. J Anim Sci. 2000;78(2):464–70.
21. Aschenbach JR, Furll B, Gabel G. Histamine affects growth of sheep ruminal epithelial cells kept in primary culture. Zentralblatt fur Veterinarmedizin Reihe A. 1998;45(6–7):411–6.
22. Sun X, Yuan X, Chen L, Wang T, Wang Z, Sun G, Li X, Li X, Liu G. Histamine induces bovine rumen epithelial cell inflammatory response via NF-κB pathway. Cell Physiol Biochem. 2017;42(3):1109–19.
23. Wang K, Sun Z, Li Y, Liu M, Loor JJ, Jiang Q, Liu G, Wang Z, Song Y, Li X. Histamine promotes adhesion of neutrophils by Inhibition of autophagy in dairy cows with subacute ruminal acidosis. J Dairy Sci. 2022;105(9):7600–14.
24. Bartell SM, Batal AB. The effect of supplemental glutamine on growth performance, development of the Gastrointestinal tract, and humoral immune response of broilers. Poult Sci. 2007;86(9):1940–7.
25. Calder PC, Yaqoob P. Glutamine and the immune system. Amino Acids. 1999;17(3):227–41.
26. Wang J, Chen L, Li P, Li X, Zhou H, Wang F, Li D, Yin Y, Wu G. Gene expression is altered in piglet small intestine by weaning and dietary glutamine supplementation. J Nutr. 2008;138(6):1025–32.
27. Ma J, Shah AM, Wang ZS, Hu R, Zou HW, Wang XY, Zhao SN, Kong XY. Dietary supplementation with glutamine improves Gastrointestinal barrier function and promotes compensatory growth of growth-retarded Yaks. Animal. 2021;15(2):100108.
28. Wang J, Hu R, Wang Z, Guo Y, Wang S, Zou H, Peng Q, Jiang Y. Establishment of Immortalized Yak Ruminal Epithelial Cell Lines by Lentivirus-Mediated SV40T and hTERT Gene Transduction. Oxidative Medicine and Cellular Longevity. 2022; 2022:8128028.
29. Kurata K, Kawahara H, Nishimura K, Jisaka M, Yokota K, Shimizu H. Skatole regulates intestinal epithelial cellular functions through activating Aryl hydrocarbon receptors and p38. Biochem Biophys Res Commun. 2019;510(4):649–55.
30. Kim D, Langmead B, Salzberg SL. HISAT: a fast spliced aligner with low memory requirements. Nat Methods. 2015;12(4):357–U121.
31. Love MI, Huber W, Anders S. Moderated Estimation of fold change and dispersion for RNA-seq data with DESeq2. Genome Biol. 2014;15(12):1–21.
32. Li Y, Yu Y, Zhao F, Zhao Z, Dou M, Cao Z, Li W, Ding K, Zhang C. Glutamine protects cow's ruminal epithelial cells from acid-induced injury. CZECH JOURNAL OF ANIMAL SCIENCE; 2024.
33. Plaizier JC, Khafipour E, Li S, Gozho GN, Krause DO. Subacute ruminal acidosis (SARA), endotoxins and health consequences. Anim Feed Sci Technol. 2012;172(1–2):9–21.
34. Ma J, Zhu Y, Wang Z, Yu X, Hu R, Wang X, Cao G, Zou H, Shah AM, Peng Q, et al. Glutamine supplementation affected the gut bacterial community and fermentation leading to improved nutrient digestibility in growth-retarded Yaks. FEMS Microbiol Ecol. 2021;97(7):fiab084.
35. Hall JC, Heel K, McCauley R, Glutamine. Br J Surg. 1996;83(3):305–12.
36. Smith RJ, Wilmore DW. Glutamine nutrition and requirements. JPEN J Parenter Enter Nutr. 1990;14(4 Suppl):S94–9.
37. Chomczynski P, Sacchi N. Single-step method of RNA isolation by acid guanidinium thiocyanate-phenol-chloroform extraction. Anal Biochem. 1987;162(1):156–9.
38. Deng Y, Cheng H, Li J, Han H, Qi M, Wang N, Tan B, Li J, Wang J. Effects of glutamine, glutamate, and aspartate on intestinal barrier integrity and amino acid pool of the small intestine in piglets with normal or low energy diet. Front Veterinary Sci. 2023;10:1202369.
39. Aschenbach JR, Zebeli Q, Patra AK, Greco G, Amasheh S, Penner GB. Symposium review: The importance of the ruminal epithelial barrier for a healthy and productive cow. Journal of Dairy Science. 2019; 102(2):1866–1882.
40. Anderson JM, Van Itallie CM. Physiology and function of the tight junction. Cold Spring Harb Perspect Biol. 2009;1(2):a002584.
41. Shen L, Weber CR, Raleigh DR, Yu D, Tumer JR, Tight. Junction Pore and Leak Pathways: A Dynamic Duo. In: Annual Review of Physiology. Edited by Julius D, Clapham DE, vol. 73; 2011: 283–309.
42. Zihni C, Mills C, Matter K, Balda MS. Tight junctions: from simple barriers to multifunctional molecular gates. Nat Rev Mol Cell Biol. 2016;17(9):564–80.
43. Capaldo CT, Powell DN, Kalman D. Layered defense: how mucus and tight junctions seal the intestinal barrier. J Mol Medicine-Jmm. 2017;95(9):927–34.
44. Graham C, Simmons NL. Functional organization of the bovine rumen epithelium. Am J Physiol Regul Integr Comp Physiol. 2005;288(1):R173–181.
45. Li M, Oshima T, Ito C, Yamada M, Tomita T, Fukui H, Miwa HJD. Glutamine blocks interleukin-13-induced intestinal epithelial barrier dysfunction. Digestion. 1964;102(2):170–9.
46. Shaghaghi H, Para R, Tran C, Roman J, Ojeda-Lassalle Y, Sun J, Romero F, Summer R. Glutamine restores mitochondrial respiration in bleomycin-injured epithelial cells. Free Radic Biol Med. 2021;176:335–44.
47. Wang J-b, Qi L-l, Zheng S-d. Wu T-x. Curcumin induces apoptosis through the mitochondria-mediated apoptotic pathway in HT-29 cells. J ZHEJIANG UNIVERSITY-SCIENCE B. 2009;10(2):93–102.

48. Liang B, Zhong Y, Huang Y, Lin X, Liu J, Lin L, Hu M, Jiang J, Dai M, Wang B et al. Underestimated health risks: polystyrene micro- and nanoplastics jointly induce intestinal barrier dysfunction by ROS-mediated epithelial cell apoptosis. Part Fibre Toxicol. 2021; 18(1).
49. Zhang B, Sun H, Sun Z, Liu N, Liu R, Zhong Q. Glutamine alleviated heat stress-induced damage of Porcine intestinal epithelium associated with the mitochondrial apoptosis pathway mediated by heat shock protein 70. J Anim Sci. 2023; 101.
50. Dhillon AS, Hagan S, Rath O, Kolch W. MAP kinase signalling pathways in cancer. Oncogene. 2007;26(22):3279–90.
51. Gehart H, Kumpf S, Ittner A, Ricci R. MAPK signalling in cellular metabolism: stress or wellness? EMBO Rep. 2010;11(11):834–40.
52. Liao T, Wen D, Ma B, Hu J-Q, Qu N, Shi R-L, Liu L, Guan Q, Li D-S, Ji Q-H. Yes-associated protein 1 promotes papillary thyroid cancer cell proliferation by activating the ERK/MAPK signaling pathway. ONCOTARGET. 2017;8(7):11719–28.
53. Adderley SP, Lawrence C, Madonia E, Olubadewo JO, Breslin JW. Histamine activates p38 MAP kinase and alters local lamellipodia dynamics, reducing endothelial barrier integrity and eliciting central movement of actin fibers. Am J PHYSIOLOGY-CELL Physiol. 2015;309(1):C51–9.

Publisher's note